Genomics, evolutionary history and diagnostics of the *Alternaria alternata* species group including apple and Asian pear pathotypes

Andrew D. Armitage[1]*, Helen M. Cockerton[1], Surapareddy Sreenivasaprasad[2], James Woodhall[3], Charles Lane[4], Richard J. Harrison[1] and John P. Clarkson[5]

[1] NIAB EMR, New Road, East Malling, Kent, ME19 6BJ, UK
[2] University of Bedfordshire, University Square, Luton, Bedfordshire, LU1 3JU, UK
[3] Parma Research and Extension Center, University of Idaho, Parma 83660, USA
[4] The Food and Environment Research Agency, Sand Hutton, York, YO41 1LZ, UK
[5] University of Warwick, Wellesbourne, Warwick, CV35 9EF, UK

*Corresponding author

E-mail: andrew.armitage@emr.ac.uk

Running head: Genomic characterization of Alternaria

Keywords: CDC, host-specific toxin, mating type, Dothideomycete, *Alternaria mali*, *Alternaria gaisen*, Oxford Nanopore

Accession numbers: Accession numbers for genomic data are provided in Table 4. Sanger sequence data is deposited on NCBI under accession numbers MK255031-MK255052.

Abstract

The *Alternaria* section *alternaria* (*A. alternata* species group) represents a diverse group of saprophytes, human allergens and plant pathogens. *Alternaria* taxonomy has benefited from recent phylogenetic revision but the basis of differentiation between major phylogenetic clades within the group is not yet understood. Furthermore, genomic resources have been limited for the study of host-specific pathotypes. We report near complete genomes of the apple and Asian pear pathotypes as well as draft assemblies for a further 10 isolates representing *Alternaria tenuissima* and *Alternaria arborescens* lineages. These assemblies provide the first insights into differentiation of these taxa as well as allowing the description of effector and non-effector profiles of apple and pear conditionally dispensable chromosomes (CDCs). We define the phylogenetic relationship between the isolates sequenced in this study and a further 23 *Alternaria* spp. based on available genomes. We determine which of these genomes represent MAT1-1-1 or MAT1-2-1 idiomorphs and designate host-specific pathotypes. We show for the first time that the apple pathotype is polyphyletic, present in both the *A. arborescens* and *A. tenuissima* lineages. Furthermore, we profile a wider set of 89 isolates for both mating type idiomorphs and toxin gene markers. Mating-type distribution indicated that gene flow has occurred since the formation of *A. tenuissima* and *A. arborescens* lineages. We also developed primers designed to *AMT14,* a gene from the apple pathotype toxin gene cluster with homologs in all tested pathotypes. These primers allow identification and differentiation of apple, pear and strawberry pathotypes, providing new tools for pathogen diagnostics.

Introduction

Species within the genus *Alternaria* encompass a range of lifestyles, acting as saprophytes, opportunistic pathogens and host-adapted plant pathogens (Thomma

2003). Large spored species include *A. solani*, a major pathogen of potato, whereas small spored taxa include the *Alternaria alternata* species group (*Alternaria* sect. *alternaria*), which are found ubiquitously in the environment acting as saprophytes and opportunistic necrotrophs. This species group is responsible for opportunistic human infections and a range of host adapted plant diseases.

Taxonomy within this presumed asexual genus has been subject to recent revision (Lawrence et al. 2013). Large spored species can be clearly resolved by standard phylogenetic markers such as ITS and are supported by morphological characters. However, small spored species within the *A. alternata* species group overlap in morphological characters, possess the same ITS haplotype (Kusaba and Tsuge, 1995a) and show low variation in other commonly used barcoding markers (Woudenberg et al. 2015; Lawrence et al. 2013; Armitage et al. 2015). Highly variable phylogenetic markers have provided resolution between groups of isolates that possess morphological patterns typical of descriptions for *A. gaisen*, *A. tenuissima* and *A. arborescens* (Armitage et al. 2015). However, taxonomy of the species group is further complicated by designation of isolates as pathotypes, each able to produce polyketide host-selective toxins (HST) adapted to apple, Asian pear, tangerine, citrus, rough lemon or tomato (Tsuge et al. 2013). Genes involved in the production of these HSTs are located on conditionally dispensable chromosomes (CDCs) (Hatta et al. 2002). CDCs have been estimated to be 1.05 Mb in the strawberry pathotype (Hatta et al. 2002), 1.1 - 1.7 Mb in the apple pathotype (Johnson et al. 2001), 1.1 - 1.9 Mb in the tangerine pathotype (Masunaka et al. 2000; Masunaka et al. 2005) and 4.1 Mb in the pear pathotype (Tanaka et al. 1999; Tanaka & Tsuge 2000). These CDCs are understood to have been acquired through horizontal gene transfer and as such, the evolutionary history of CDCs may be distinct from the core genome.

The polyketide synthase genes responsible for the production of the six HSTs are present in clusters. Some genes within these clusters are conserved between pathotypes (Miyamoto et al. 2009; Hatta et al. 2002), while genes are also present within these clusters that are unique to particular pathotypes (Ajiro et al. 2010;

Miyamoto et al. 2010). This is reflected in structural similarities between the pear (AKT) and strawberry (AFT) and tangerine (ACTT) toxins with each containing a 9,10-epoxy-8-hydroxy-9-methyl-decatrienoic acid moiety. In contrast, the toxin produced by the apple pathotype (AMT) does not contain this moiety and is primarily cyclic in structure (Tsuge et al. 2013).

Studies making use of bacterial artificial chromosomes (BAC) have led to the sequencing of toxin gene cluster regions from three apple pathotype isolates (Genbank accessions: AB525198, AB525199, AB525200; unpublished). These sequences are 100-130 Kb in size and contain 17 genes that are considered to be involved in synthesis of the AMT apple toxin (Harimoto et al. 2007). *AMT1*, *AMT2*, *AMT3* and *AMT4* have been demonstrated to be involved in AMT synthesis, as gene disruption experiments have led to loss of toxin production and pathogenicity (Johnson et al. 2000; Harimoto et al. 2007; Harimoto et al. 2008). However, experimental evidence has not been provided to show that the remaining 13 *AMT* genes have a role in toxin production. Four genes present in the CDC for the pear pathotype have been identified and have been named *AKT1*, *AKT2*, *AKT3*, *AKTR-1* (Tanaka et al. 1999; Tanaka & Tsuge 2000; Tsuge et al. 2013) and a further two genes (*AKT4*, *AKTS1*) have been reported (Tsuge et al. 2013).

The toxicity of a HST is not restricted to the designated host for that pathotype. All or some of the derivatives of a toxin may induce necrosis on “non-target” host leaves. For example, AMT from the apple pathotype can induce necrosis on the leaves of Asian pear (Kohmoto et al. 1976). Therefore non-host resistance may be triggered by recognition of non-HST avirulence genes.

Alternaria spp. are of phytosanitary importance, with apple and pear pathotypes subject to quarantine regulations in Europe (Smith et al. 1997). As such, rapid and accurate diagnostics are required for identification. Where genes on essential chromosomes can be identified that phylogenetically resolve taxa, then these can be used for identification of quarantine pathogens (Bonants et al. 2010; Quaedvlieg et al. 2012). Regulation and management strategies also need to consider the potential for genetic exchange

between species. The *Alternaria* sect. *alternaria* are presumed asexual but evidence has been presented for either the presence of sexuality or a recent sexual past. Sexuality or parasexuality provides a mechanism for reshuffling the core genome associated with CDCs of a pathotype. It is currently unknown whether pathotype identification can be based on sequencing of phylogenetic loci, or whether the use of CDC-specific primers is more appropriate. This is of particular importance for the apple and Asian pear pathotypes due the phytosanitary risk posed by their potential establishment and spread in Europe.

Results

Twelve genomes were sequenced, selected from a collection of isolates whose phylogenetic identity was determined in previous work (Armitage et al. 2015). These twelve isolates were three *A. arborescens* clade isolates (FERA 675, RGR 97.0013 and RGR 97.0016), four *A. tenuissima* clade isolates (FERA 648, 1082, 1164 and 24350), three *A. tenuissima* clade apple pathotype isolates (FERA 635, 743, 1166 and 1177) and one *A. gaisen* clade pear pathotype isolate (FERA 650).

Generation of near-complete genomes for the apple and pear pathotype using MinION sequencing

Assemblies using nanopore long-read sequence data for the apple pathotype isolate *FERA 1166*, and pear pathotype isolate *FERA 650* were highly contiguous, with the former totaling 35.7 Mb in 22 contigs and the latter totaling 33.6 Mb in 23 contigs (Table 1). Whole genome alignments of these assemblies to the 10 chromosomes of *A. solani* showed an overall macrosynteny between genomes (Fig. 1), but with structural rearrangement of apple pathotype chromosomes in comparison to *A. solani* chromosomes 1 and 10. The Asian pear pathotype had distinct structural rearrangements in comparison to *A. solani*, chromosomes 1 and 2 (Fig. 1). Scaffolded contigs of *FERA 1166* spanned the entire length of *A. solani* chromosomes 2, 3, 6, 8 and 9 and chromosomes 4, 5, 6 and 10 of *FERA 650* (Fig. 1). Interestingly, sites of

major structural rearrangements within *A. solani* chromosome 1 were flanked by telomere-like TTAGGG sequences.

Genome assembly of 10 Illumina sequenced isolates yielded assemblies of a similar total size to MinION assemblies (33.9 - 36.1 Mb) but fragmented into 167-912 contigs. Assembled genomes were repeat sparse, with 1.41 - 2.83 % of genomes repeat masked (Table 1). Genome assemblies of *A. arborescens* isolates (33.8 - 33.9 Mb), were of similar total size to non-pathotype *A. tenuissima* isolates and had similar repetitive content (2.51 – 2.83 and 1.41 – 2.83 % respectively). Despite this, identification of transposon families in both genomes showed expansion of DDE (T_{5df} = 5.36, P > 0.01) and gypsy (T_{5df} = 6.35, P > 0.01,) families in *A. arborescens* genomes (Fig. 2).

Phylogeny of sequenced isolates

The relationship between the 12 sequenced isolates and 23 *Alternaria* spp. with publically available genomes was investigated through phylogenetic analysis of 500 shared core ascomycete genes. *A. pori* and *A. destruens* genomes were excluded from the analysis due to low numbers of complete single copy ascomycete genes being found in their assemblies (Supp. information 1). The 12 sequenced isolates were distributed throughout *A. gaisen*, *A. tenuissima* and *A. arborescens* clades (Fig. 3). The resulting phylogeny (Fig. 3), formed the basis for later assessment of CDC presence and mating type distribution among newly sequenced and publicly available genomes, as discussed below.

Gene and effector identification

Gene prediction resulted in 12757 – 13733 genes from the our assemblies (Table 1), with significantly more genes observed in the apple pathotype isolates than in *A. tenuissima* clade non-pathotype isolates (P > 0.01, $F_{2,8df}$ = 51.19). BUSCO analysis identified that gene models included over 97% of the single copy conserved ascomycete genes, indicating well trained gene models. Apple pathotype isolates

possessed greater numbers of secondary metabolite clusters ($P > 0.01$, $F_{2,8df} = 8.96$) and secreted genes ($P > 0.01$, $F_{2,8df} = 44.21$) than non-pathotype *A. tenuissima* isolates, indicating that CDCs contain additional secreted effectors. Non-pathotype *A. tenuissima* clade isolates were found to possess greater numbers of genes encoding secreted proteins than *A. arborescens* isolates ($P > 0.01$, $F_{2,8df} = 44.21$), including secreted CAZYmes ($P > 0.01$, $F_{2,8df} = 9.83$). The basis of differentiation between these taxa was investigated further.

Genomic differences between *A. tenuissima* and *A. arborescens* clades

Orthology analysis was performed upon the combined set of 158,280 total proteins from the 12 sequenced isolates. In total, 99.2 % of proteins clustered into 14,187 orthogroups. Of these, 10,669 orthogroups were shared between all isolates, with 10,016 consisting of a single gene from each isolate. This analysis allowed the identification of 239 orthogroups that were either unique to *A. arborescens* isolates or expanded in comparison to non-pathotype *A. tenuissima* isolates.

Expanded and unique genes to *A. arborescens* isolates was further investigated using *FERA 675* (Supp. information 2). Genes involved in reproductive isolation were in this set, including 21 of the 148 heterokayon incompatibility (HET) loci from *FERA 675*. CAZymes were also identified within this set, three of which showed presence of chitin binding activity and the other three having roles in xylan or pectin degradation. In total, 25 genes encoding secreted proteins were within this set, secreted proteins with pathogenicity-associated functional annotations included a lipase, a chloroperoxidase, an aerolysin-like toxin, a serine protease and an aspartic peptidase. A further six secreted genes had an effector-like structure by EffectorP but no further functional annotations. Furthermore, one gene from this set was predicted to encode a fungal-specific transcription factor unique to *A. arborescens* isolates.

Further to the identification of genes unique or expanded in *A. arborescens*, 220 orthogroups were identified as unique or expanded in the *A. tenuissima*. These orthogroups were further investigated using isolate *FERA 648* (Supp. information 2). This set also contained genes involved in reproductive isolation, including nine of the 153 from *FERA 648*. CAZymes within the set included two chitin binding proteins, indicating a divergence of LysM effectors between *A. tenuissima* and *A. arborescens* lineages. The five additional CAZymes in this set represented distinct families from those expanded/unique in *A. arborescens*, including carboxylesterases, chitooligosaccharide oxidase and sialidase. In total, 18 proteins from this set were predicted as secreted, including proteins with cupin protein domains, leucine rich-repeats, astacin family peptidase domains and with four predicted to have effector-like structures but no further annotations. *A. tenuissima* isolates had their own compliment of transcription factors, represented by four genes within this set.

Identification and characterisation of CDC regions within *A. alternata* apple and Asian pear pathotypes

Identification of CDC contigs and assessment of copy number

Alignment of Illumina reads to the apple and Asian pear pathotype MinION reference assemblies identified variable presence of some contigs, identifying these as contigs representing CDCs (CDC contigs) (Table 2). Six contigs totaling 1.87 Mb were designated as CDCs in the apple pathotype reference and four contigs totaling 1.47 Mb designated as CDCs in the pear pathotype reference. Two *A. tenuissima* clade non-pathotype isolates (FERA 1082, FERA 1164) were noted to possess apple pathotype CDC contigs 14 and 19 totaling 0.78 Mb (Table 2).

Read alignments showed that CDC contigs were present in multiple copies within *A. alternata* pathotype isolates. *FERA 1166* Illumina reads aligned to its own assembly showed two-fold coverage over contigs 14, 15, 20 and 21 in comparison to core contigs

(Table 2). This was more pronounced in isolate *FERA 1177* that had between two- and eight-fold coverage of these contigs. The same was observed in pear pathotype CDC regions, with contigs 14 and 24 in isolate *FERA 650* showing two-fold coverage from Illumina reads in comparison to core contigs.

Toxin gene clusters are present on multiple CDC contigs

Homologs to 15 of the 17 AMT cluster genes were located on contigs 20 and 21 in the apple pathotype reference genome (e-value < $1x10^{-30}$, > 70% query alignment), confirming them as CDC-regions (Table 3). Of the remaining two genes, *AMT11* had low-confidence BLAST homologs on contigs 18 and 21 (e-value < $1x10^{-30}$) whereas the best BLAST hit of *AMT15* was located on contig 18 (e-value < $1x10^{-30}$). Duplication of toxin gene regions was observed between CDC contigs, with contig 20 carrying homologs to 16 toxin genes, but with contig 21 also carrying the *AMT1* to *AMT12* section of the cluster (Table 3). The three other apple pathotype isolates (FERA 635, 743 and 1177) also showed presence of 15 of the 17 AMT genes (e-value < $1x10^{-30}$, > 70% query alignment), and with some AMT genes present in multiple copies within the genome indicating that the AMT toxin region has also been duplicated in these isolates.

The Asian pear pathotype was also found to carry toxin gene clusters in multiple copies, with homologs to the four AKT cluster genes present on contig 14 of the FERA 650 assembly (e-value < $1x10^{-30}$, > 70% query alignment), with three of these also present on contig 24 (e-value < $1x10^{-30}$, two with > 70% query alignment). BLAST hit results from AKT genes were supported by their homologs from strawberry and tangerine pathotypes also found in these regions (Table 3). The pear pathotype genome was also found to contain additional homologs from apple (*AMT14*), strawberry (*AFT9-1*, *AFT10-1*, *AFT11-1* and *AFT12-1*) and citrus (*ACTT5* and *ACTT6*) located on CDC contigs 14 and 24 (Table 3).

Characterisation of core and CDC effector profiles

A total of 624 proteins were encoded on the six contigs designated as CDCs in the reference apple pathotype genome, with 502 proteins encoded on the four Asian pear pathotype CDC contigs (Supp. information 3). We further investigated the gene complements of these regions.

Approximately a quarter of gene models on apple pathotype CDC contigs were involved in secondary metabolism, with 153 genes present in six secondary metabolite gene clusters. This included AMT toxin gene homologs on contigs 20 and 21, which were located within NRPS secondary metabolite gene clusters. Three other secondary metabolite clusters were located on CDC contigs with two of these involved in the production of T1PKS secondary metabolites and the third with unknown function. A further two secondary metabolite clusters were located on contig 14 shared with two non-pathotype isolates, one of which is involved in the production of a T1PKS. The pear pathotype also carried 153 genes in secondary metabolite gene clusters. These 30 % of CDC genes were located in four clusters, with the AKT toxin genes in T1PKS clusters of contigs 14 and 24. A second cluster was present on contig 14 with unknown function and a T1PKS cluster was present on contig 16.

Approximately 5 % of the genes on apple CDC contigs encoded secreted proteins, with 32 in isolate *FERA 116*6 many of which had potential effector functions with six designated as CAZymes and 12 testing positive by EffectorP. Similarly, a total of 41 secreted proteins were predicted on the CDC regions of the Asian pear pathotype, with eight of these designated as secreted CAZymes and 13 testing positive by EffectorP. Further investigation into the 32 secreted proteins from the apple pathotype identified three CAZYmes from the chitin-active AA11 family, two from the cellulose-active GH61 family and one cellulose-active GH3 family protein. Six of the 13 EffectorP proteins also had domains identifiable by interproscan: four carried NTF2-like domains, which are envelope proteins facilitating protein transport into the nucleus; one was a fungal hydrophobin protein; one was a member of an panther superfamily PTHR40845 that shares structural similarity with proteins from the plant pathogens *Phaeospharia*

nodorum, *Sclerotinia sclerotiorum* and *Ustilago maydis*. Of the 38 secreted proteins identified from the pear pathotype, two CAZYmes were also identified from the chitin-active AA11 family, two from the AA3 family with single proteins from GH5, CBM67 and AA7 families. Ten of the twelve secreted EffectorP proteins had no functional information as predicted by interproscan, with the other two identified as carrying WSC domains IPR002889, which are cysteine-rich domains involved carbohydrate binding. CDCs may also play important roles in transcriptional regulation with 29 putative transcription factors identified in the apple pathotype CDC contigs(4.6 % CDC genes) and 35 identified in pear pathotype CDC contigs (7.0 % CDC genes).

Distribution of isolates carrying AMT and AKT genes

The evolutionary relationship between *A. alternata* pathotypes sequenced in this study and publicly available genomes was analyzed by the core gene phylogeny (Fig. 2). We identified four isolates as tangerine pathotypes (Z7, BMP2343, BMP2327, BMP3436) two as tomato pathotypes (BMP0308, EGS39-128), one Asian pear pathotype (MBP2338), one rough-lemon (BMP2335) and two apple pathotypes (BMP3063, BMP3064) through searches for genes from HST-gene clusters (Supp. information 4). When plotted on the genome phylogeny, we found the apple and tangerine pathotypes to be polyphyletic (Fig. 2). Five of the six sequenced apple pathotype isolates were located in the *A. tenuissima* clade and one in the *A. arborescens* clade, whereas the tangerine pathotype was present in both the *A. tenuissima* clade and in the *A. tangelonis / A. longipes* clade.

PCR primers for three loci *(AMT4*, *AKT3* and *AMT14*) were designed to identify the distribution of pathotypic isolates through the *A. alternata* species group and were screened against a set of 89 previously characterised isolates (Fig. 4). Five isolates tested positive for the presence of *AMT4*, each of which was from the *A. tenuissima* clade (FERA 635, FERA 743, FERA 1166, FERA 1177). Five isolates tested positive for the presence of *AKT3*, including the three isolates from Asian pear in the *A. gaisen* clade and a further two isolates from the *A. tenuissima* clade that were from strawberry.

Sequencing of the *AKT3* amplicons from the two isolates *ex.* strawberry identified them as the *AFT3-2* ortholog of *AKT3*, showing that these isolates were strawberry pathotypes rather than pear pathotypes. Sequencing of PCR products from the other isolates confirmed them to be apple or pear pathotypes as expected. All of the isolates testing positive for *AMT4* or *AKT3* also tested positive for *AMT14*, indicating its suitability as a target gene for identification of a range of pathotypes.

Presence of apple pathotype CDCs was confirmed to be associated with pathogenicity through detached apple leaf assays. Apple pathotype isolates showed significantly greater numbers of necrotic lesions when inoculated onto *cv.* Spartan (F_{72df} =100.64) and *cv.* Bramley's Seedling (F_{72df} =69.64) leaves than non-pathotype *A. tenuissima* isolates (Fig. 5).

Signatures of genetic exchange

Mating type distributions

Of the 12 sequenced isolates, BLAST searches identified five as carrying the MAT1-1-1 idiomorph and seven as carrying MAT1-2-1. Both idiomorphs showed distribution throughout the *A. alternata* genome phylogeny (Fig. 2). These results were supported by PCR assays identifying the mating type of 89 previously characterised isolates (Fig. 4). Idiomorphs did not deviate from a 1:1 ratio within *A. tenuissima* (21 MAT1-1-1 : 23 MAT1-2-1; $\chi2$ = 0.09, 1df, P>0.05) or *A. arborescens* clades (18 MAT1-1-1 : 24 MAT1-2-1; $\chi2$ = 0.86; 1df; P>0.05), as expected under a random mating population. All three of the *A. gaisen* clade isolates carried the MAT1-2-1 idiomorph.

Genomic signatures of recombination

Signatures of recombination were searched for through calculating rate of linkage decay within the *A. tenuissima* and *A. arborescens* isolates as well as by identifying genes that are putative sites of recombination using the four gamete test. Assessment of SNP linkage of both lineages found low levels of linkage decay as pairwise SNP distance increased. Notably, LD50 was not reached at pairwise SNP distances of 1 Mb apart,

indicative of a lack of recombination, or a genetically homogeneous population. In contrast, the four gamete test identified 89 genes (of 4708 containing multiple SNPs) with patterns typical of a single recombination event and a further five genes showing patterns typical of two recombination events.

Discussion

This work builds upon the current genomic resources available for *Alternaria*, including the *A. brassicicola* and *A. solani* genomes (Belmas et al. 2018; Wolters et al. 2018), *A. alternata* from onion (Bihon et al. 2016) the additional 25 *Alternaria spp.* genomes available on the *Alternaria* Genomes Database (Dang et al. 2015) as well as recent genomes for other pathotype and non-pathotype *A. alternata* (Hou et al. 2016; Wang et al. 2016; Nguyen et al. 2016). Of the previously sequenced genomes, *A. solani*, the citrus pathotype and a non-pathotype *A. alternata* isolate have benefitted from long read sequencing technology with each comprising less than 30 contigs (Wolters et al. 2018; Wang et al. 2016; Nguyen et al. 2016). Total genome sizes in this study (33-36 Mb) were in line with previous estimates for *A. alternata*, with the tomato pathotype also previously assembled into 34 Mb (Hu et al. 2012). Synteny analysis of our two reference genomes against the chromosome-level *A. solani* genome revealed structural differences for chromosomes 1 and 10 in the apple pathotype and for chromosomes 1 and 2 in the pear pathotype. These structural differences may represent distinct traits between clades of the *A. alternata* species group, and may represent a barrier to genetic exchange involved in the divergence of *A. gaisen* and *A. tenuissima* lineages. The number of essential chromosomes in our reference genomes is in line with previous findings in *A. alternata* (Kodama et al. 1998), with 9-11 core.

Species designations within the species group have been subject to recent revision (Woudenberg et al. 2015; Lawrence et al. 2013; Armitage et al. 2015) leading to potential confusion when selecting isolates for study. For example, the available *A. fragariae* genome (Dang et al. 2015), did not represent a strawberry pathotype isolate and was located in the *A. gaisen* clade. As such, the phylogenetic context for sequenced *Alternaria* genomes described in this study, along with pathotype identification provides a useful framework for isolate selection in future work.

Evidence of genetic exchange

A 1:1 ratio of MAT loci was observed within *A. arborescens* and *A. tenuissima* clades. This supports previous identification of both idiomorphs within *A. alternata, A. brassicae* and *A. brassicicola* (Berbee et al. 2003). Furthermore, presence of both MAT idiomorphs within apple pathotype isolates indicates that genetic exchange (sexuality or parasexuality) has occurred since the evolution of CDCs, providing a mechanism of transfer of CDCs. Furthermore, we show that some recent or historic genetic exchange has occurred between *A. tenuissima* and *A. arborescens* clades, with both apple and tangerine pathotypes exhibiting a polyphyletic distribution throughout the phylogeny.

The Four Gamete test is capable of detecting rare recombination within populations (Stumpf & McVean 2003) and has previously provided evidence of recombination within a citrus brown spot population of *A.* sect. *alternaria* (Stewart et al. 2013). We did not see signatures of linkage decay, indicative of a highly homogeneous population, or one with infrequent recombination. The nature of genetic exchange cannot be distinguished by these methods (Nieuwenhuis & James 2016), and may be sexual or parasexual. However, maintenance of both MAT idiomorphs in a 1:1 ratio within *A. tenuissima* and *A. arborescens* clades supports a functional role of the MAT loci and thus sexuality.

Duplication of toxin-gene contigs

Toxin genes have been proposed to be present in multiple copies within *A.* sect. *alternaria* pathotype genomes with *AMT2* proposed to be present in at least three copies in the apple pathotype CDC (Harimoto et al. 2008), and multiple copies of *AKTR* and *AKT3* in the pear pathotype (Tanaka et al. 1999; Tanaka & Tsuge 2000). Through read mapping we demonstrated that this is the case. Furthermore, we show that toxin gene clusters are present on multiple contigs, with differences in the gene complements between these clusters. At this stage, it is unclear whether these different clusters are responsible for the production of the variant R-groups previously characterised in AMT or AKT toxins (Nakashima et al. 1985; Harimoto et al. 2007). Differences were also noted between non-pathotype isolates from the *A. tenuissima* clade in the presence/absence of contigs 14 and 19, representing a total of 775 Kb. Chromosomal

loss has been reported in the apple pathotype (Johnson et al. 2001), and it is not clear if this represents chromosomal instability in culture or additional dispensable chromosomes within *A. tenuissima* clade isolates.

PCR primers for diagnostics

It is now clear that genes on essential chromosomes do not provide reliable targets for identification of different pathotypes and hence loci located directly on CDCs should be used. We found *AMT14* homologs to be present in all pathotype genomes and designed primers to this region. These demonstrated specificity to apple, pear and strawberry pathotypes within a set of 86 *Alternaria* isolates. Furthermore, Sanger sequencing of these amplicons confirmed this to be a single locus that can both identify and discriminate a range of pathotypes. Wider validation of this primer set is now required to test its suitability across other pathotypes.

Divergence of *A. arborescens* and *A. tenuissima*

The divergence of *A. tenuissima* and *A. arborescens* lineages was investigated through identification of expanded and unique gene compliments. We identified HET loci unique to *A. arborescens* or *A. tenuissima* lineages. HET loci may act as incompatibility barriers to common genetic exchange between these taxa (Glass & Kaneko 2003). Taxa also showed divergence in effector profiles, including chitin binding effectors, with *A. arborescens* isolates possessing unique xylan/pectin degradation CAZymes, while *A. tenuissima* isolates possessed unique carboxylesterase, chitooligosaccharide and sialidase CAZymes. Chitin binding proteins are important in preventing MAMP triggered host recognition by plants and animals during infection, and may also aid persistence of resting bodies outside of the host (Kombrink & Thomma 2013). Putative transcription factors were also amongst the proteins specific to *A. arborescens* or *A. tenuissima*, indicating that these taxa not only possess distinct gene complements but also differ in how they respond to stimuli. Dispersed repeat sequences such as transposable elements have been shown to serve as sites of recombination within and between fungal chromosomes (Zolan 1995) and we also show distinct transposon profiles between *A. arborescens* and *A. tenuissima*. Transposons are known to aid host

adaptation in plant pathogens (Faino et al. 2016; Gijzen 2009; Schmidt et al. 2013) and have been a mechanism for differentiation of these taxa.

Other effectors on CDC regions

Alternaria HSTs are capable of inducing necrosis on non-host leaves (Kohmoto et al. 1976), meaning that non-host resistance must be associated with recognition of other avirulence genes. We investigated the complements of other putative pathogenicity genes and effectors produced by the apple and Asian pear pathotypes and identified additional CAZymes and secondary metabolite profiles on CDC regions, distinct between pathotypes, suggesting additional host-adapted tools for pathogenicity. Additional secondary metabolites clusters were present on both apple and pear pathotype CDCs as well as unique complements of secreted CAZymes. CAZyme families AA3, AA7 and AA9 have previously been reported to be in greater numbers in the citrus pathotype in comparison to non-pathotypes (Wang et al. 2016). Furthermore, putative transcription factor genes were identified in CDCs indicating that these regions may have some level of transcriptional autonomy from the core genome. This has been shown in *Fusarium*, where effector proteins are regulated by the SGE transcription factor on the core genome but also by FTF and other transcription factor families (TF1-9) located on lineage specific chromosomes (van der Does et al. 2016).

Conclusions

We report near-complete reference genomes for the apple and Asian pear pathotypes of *A.* sect. *alternaria* and provide genomic resources for a further ten diverse isolates from this clade. For the first time we show sequenced *Alternaria* genomes in a phylogenetic context allowing the identification of both mating type idiomorphs present in arborescens and tenuissima clades, with a distribution throughout subclades that was indicative of recent genetic exchange. The presence of the apple pathotype in isolates of both mating types supports gene flow between isolates. Furthermore, the distribution of isolates from different pathotypes throughout the phylogeny indicated that apple and tangerine pathotypes are polyphyletic. This means that gene flow is not limited to within, but has also occurred between *A. tenuissima* and *A. arborescens* lineages. We also

developed PCR primers to aid identification of pathotypes, with those targeting the AMT14 locus identifying a range of pathotypes due to its conservation between CDCs. Despite evidence of genetic exchange between *A. arborescens* and *A. tenuissima* clades, we show that these taxa are sufficiently isolated to have diverged, with significant differences in core effector profiles and transposon content.

Experimental Procedures

DNA and RNA extraction and sequencing

Apple pathotype isolate *FERA 1166* and Asian pear pathotype isolate *FERA 650* were sequenced using both Illumina and nanopore MinION sequencing technologies and the remaining ten isolates were sequenced using Illumina sequencing technology. Detailed methodology for extraction and sequencing of DNA and RNA are provided in Supp. information 5. MinION sequencing generated 39 and 44 times coverage for isolates *FERA 1166* and *FERA 650*, respectively. Whereas paired-end Illumina sequencing generated 24-76 times coverage for the 12 isolates. RNAseq was performed to aid training of gene models, with RNA generated from isolates *FERA 1166* and *FERA 650* grown in full strength PDB, 1% PDB, Potato Carrot Broth (PCB) and V8 juice broth (V8B). With libraries pooled by isolate and sequenced using paired-end Illumina sequencing.

Genome assembly and annotation

De-novo genome assembly was performed for all 12 isolates. Assemblies for isolates *FERA 1166* and *FERA 650* were generated using SMARTdenovo (https://github.com/ruanjue/smartdenovo). Prior to assembly adapters were removed from MinION reads using Porechop v0.1.0 and reads were further trimmed and corrected using Canu v1.6 (Ruan 2016; Koren et al. 2017). Following initial assembly, contigs were corrected using MinION reads through ten rounds of Racon (May 29, 2017 github commit) correction (Vaser et al. 2017) and one round of correction using MinION signal information with nanopolish (v0.9.0) (Loman et al. 2015). Final correction was performed through ten rounds of Pilon v1.17 (Walker et al. 2014) using Illumina sequence data. Assemblies for the ten isolates with Illumina-only data were generated using Spades v.3.11.0 (Bankevich et al. 2012). Assembly quality statistics were summarized using Quast v.4.5 (Gurevich et al. 2013). Single copy core Ascomycete genes were identified within the assembly using BUSCO v3 and used to assess assembly completeness (Simão et al. 2015). RepeatModeler, RepeatMasker and

TransposonPSI were used to identify repetitive and low complexity regions (http://www.repeatmasker.org, http://transposonpsi.sourceforge.net). Visualisation of whole genome alignments between *FERA 1166* and *FERA 650* was performed using circos v0.6, following whole genome alignment using the nucmer tool as part of the MUMmer package v4.0.

Gene prediction was performed on softmasked genomes using Braker1 v.2 (Hoff et al. 2016), a pipeline for automated training and gene prediction of AUGUSTUS 3.1 (Stanke & Morgenstern 2005). Additional gene models were called in intergenic regions using CodingQuarry v.2 (Testa et al. 2015). Braker1 was run using the “fungal” flag and CodingQuarry was run using the “pathogen” flag. RNAseq data generated from FERA 1166 and FERA 650 were aligned to each genome using STAR v2.5.3a (Dobin et al. 2013), and used in the training of Braker1 and CodingQuarry gene models. Orthology was identified between the 12 predicted proteomes using OrthoMCL v.2.0.9 (Li et al. 2003) with an inflation value of 5.

Draft functional genome annotations were determined for gene models using InterProScan-5.18-57.0 (Jones et al. 2014) and through identifying homology (BLASTP, E-value > $1x10^{-100}$) between predicted proteins and those contained in the March 2018 release of the SwissProt database (Bairoch & Apweiler 2000). Putative secreted proteins were identified through prediction of signal peptides using SignalP v.4.1 and removing those predicted to contain transmembrane domains using TMHMM v.2.0 (Käll et al. 2004; Krogh et al. 2001). Additional programs were used to provide evidence of effectors and pathogenicity factors. EffectorP v1.0 was used to screen secreted proteins for characteristics of length, net charge and amino acid content typical of fungal effectors (Sperschneider et al. 2016). Secreted proteins were also screened for carbohydrate active enzymes using HMMER3 (Mistry et al. 2013) and HMM models from the dbCAN database (Huang et al. 2018). DNA binding domains associated with transcription factors (Shelest 2017) were identified along with two additional fungal-specific transcription factors domains (IPR007219 and IPR021858). Annotated

assemblies were submitted as Whole Genome Shotgun projects to DDBJ/ENA/Genbank (Supp. information 6).

Phylogenetics

BUSCO hits of single copy core ascomycete genes to assemblies were extracted and retained if a single hit was found in all of the 12 sequenced genomes and 23 publically available *Alternaria* spp. genomes from the Alternaria genomes database (Dang et al. 2015). Sequences from the resulting hits of 500 loci were aligned using MAFFT v6.864b (Katoh & Standley 2013), before alignments were trimmed using trimAl v1.4.1 (Capella-Gutiérrez et al. 2009), and trees calculated for each locus using RAxML v8.1.17 (Liu et al. 2011). The most parsimonious tree from each RAxML run was used to determine a single consensus phylogeny of the 500 loci using ASTRAL v5.6.1 (Zhang et al. 2018). The resulting tree was visualised using the R package GGtree v1.12.4 (Yu et al. 2016).

CDC identification

Contigs unique to apple and pear pathotypes were identified through read alignment to assembled genomes. Read alignment was performed using Bowtie2 (Langmead & Salzberg 2012), returning a single best alignment for each paired read. Read coverage was quantified from these alignments using Samtools (Li et al. 2009).

Searches for toxin-synthesis genes in *Alternaria* genomes

Sequence data for 40 genes located in *A. alternata* HST gene clusters were downloaded from Genbank (accession numbers in Table 3). BLASTn searches were performed for all 40 gene sequences against one another to identify homology between these sequences. Genes were considered homologous where they had > 70 % identical sequences over the entire query length, and an e-value of $1x10^{-30}$. tBLASTx was used to search for the presence of these genes in assemblies.

Variant calling

SNP variants from all isolates were identified following read alignment to the *FERA 1166* genome using Bowtie2. Multi-mapping, discordant and duplicate reads were removed from alignments before SNPs were called using GATK (McKenna et al. 2010). SNPs were filtered based upon quality thresholds, using default options of the vcflib tool vcffilter (https://github.com/vcflib/vcflib). SNP effects on gene models were determined using snpEff (Cingolani et al. 2012).

Signatures of genetic exchange

Mating type idiomorphs present in publicly available genomes were identified using BLASTn searches. A wider assessment within 89 characterised *Alternaria* isolates (Armitage et al. 2015) was undertaken using specific PCR primers (Arie et al. 2000). PCR primers (AAM1-3: 5'-TCCCAAACTCGCAGTGGCAAG-3'; AAM1-3: 5'-GATTACTCTTCTCCGCAGTG-3; M2F: 5'-AAGGCTCCTCGACCGATGAA-3; M2R: 5'-CTGGGAGTATACTTGTAGTC-3) were run in multiplex with PCR reaction mixtures consisting of 10 µl redtaq (REDTaq ReadyMix PCR Reaction Mix, Sigma-Aldrich), 2 µl DNA, 1 µl of each primer (20 µM), and 4 µl purified water (Sigma-Aldrich). PCR reaction conditions comprised of an initial 60 second denaturing step at 94°C followed by 30 cycles of a melting step of 94°C for 30 seconds, an annealing step at 57°C for 30 seconds, and an extension step at 72°C for 60 seconds, these cycles were followed by a final extension step at 72°C for 420 seconds. MAT1-1-1 or MAT1-2-1 idiomorphs were determined through presence of a 271 or 576 bp product following gel electrophoresis, repectively.

SNP variants were used to calculate decay in linkage disequilibrium. Linkage was calculated using vcftools (Danecek et al. 2011), generating R^2 values representing linkage of SNPs up to 1 Mb apart. A non-linear model for linkage decay was fitted to the data to calculate the point at which linkage decayed to 50 % of the maximum value (LD50). SNP variants were also used to identify genes that showed signatures of recombination using the Four-Gamete test. This was implemented using the R PopGenome package (Pfeifer et al. 2014).

PCR screens for apple and pear toxin-synthesis genes

A set of 90 previously characterised isolates was used to further investigate the distribution of pathotypes throughout the *A. alternata* species group. PCR primers were designed for the amplification of three genes (*AMT4*, *AMT14*, *AKT3*) located within CDC gene clusters involved in toxin synthesis. Primers for *AMT4* were designed to amplify apple pathotype isolates, *AKT3* to amplify pear pathotype isolates and *AMT14* to identify both apple and pear pathotype isolates. These primers were then used to screen isolates for the presence of these genes in 30 cycles of PCR using 0.25 ul Dream taq, 1 ul of 10x PCR buffer, 1 ul of dNTPs, 1 ul of gDNA, 1 ul of each primer (5 µM), and 4.75 ul purified water (Sigma-Aldrich). PCR products were visualised using gel electrophoresis and amplicon identity confirmed through Sanger sequencing. Primers AMT4-EMR-F (5'-CTCGACGACGGTTTGGAGAA-3) and AMT4-EMR-R (5'-TTCCTTCGCATCAATGCCCT-3) were used for amplification of AMT4. Primers AKT3-EMR-F (5'-GCAATGGACGCAGACGATTC-3) and AKT3-EMR-R (5'-CTTGGAAGCCAGGCCAACTA-3) were used for amplification of *AKT3*. Primers AMT14-EMR-F (5'-TTTCTGCAACGGCGKCGCTT-3) and AMT14-EMR-R (5'-TGAGGAGTYAGACCRGRCGC-3) were used for amplification of *AMT14*. PCR reaction conditions were the same as described above for mating type loci, but with annealing performed at 66°C for all primer pairs.

Virulence assay

Pathogenicity assays were performed on apple *cv.* Spartan and *cv.* Bramley's seedling to determine differences in isolate virulence between *A. tenuissima* isolates possessing the apple pathotype CDC (*FERA 635*, *743* or *1166*) and non-pathotype isolates lacking the CDC (*FERA 648*, *1082* or *1164*). Detailed pathogenicity assay methods are provided in supplementary information 5. Briefly, leaves were inoculated with 10 ul of $1x10^5$ spore suspensions at six points and the number of leaf spots counted at 14 days post inoculation. One isolate was infected per leaf, with 10 replicates per cultivar. Binomial regression using a generalised linear model (GLM) was used to analyse the number of resulting lesions per leaf.

Acknowledgements

Dr. A.D. Armitage acknowledges the support of a Defra Plant Health Taxonomic fellowship. Thanks are given to the Food and Environmental Research Agency (UK), Dr. P. Gannibal, Dr. R. Roberts and Dr. E. Simmons for access to *Alternaria* isolates.

Bibliography

Adachi, Y., et al., 1996. Relationships between genetic polymorphisms and fungicide resistance within *Alternaria alternata. Phytopathology*,*86*(11),1248-1254.

Ajiro, N. et al., 2010. Role of the host-selective ACT-toxin synthesis gene ACTTS2 encoding an enoyl-reductase in pathogenicity of the tangerine pathotype of Alternaria alternata. Phytopathology, 100(2), pp.120–126.

Arie, T. et al., 2000. Mating-type genes from asexual phytopathogenic ascomycetes Fusarium oxysporum and Alternaria alternata. Molecular Plant-Microbe Interactions, 13(12), pp.1330–1339.

Armitage, A.D. et al., 2015. Discrete lineages within Alternaria alternata species group: Identification using new highly variable loci and support from morphological characters. *Fungal Biology, 119(11), pp.994–1006.*

Bairoch, A. & Apweiler, R., 2000. The SWISS-PROT protein sequence database and its supplement TrEMBL in 2000. Nucleic Acids Research, 28(1), pp.45–48.

Bankevich, A. et al., 2012. SPAdes: a new genome assembly algorithm and its applications to single-cell sequencing. Journal of Computational Biology, 19(5), pp.455–477.

Belmas, E. et al., 2018. Genome sequence of the necrotrophic plant pathogen Alternaria brassicicola Abra43. *Genome Announcements, 6(6).*

Berbee, M.L. et al., 2003. Shared ITS DNA substitutions in isolates of opposite mating type reveal a recombining history for three presumed asexual species in the filamentous ascomycete genus Alternaria. Mycological Research, 107(Pt 2), pp.169–182.

Bihon, W. et al., 2016. Draft Genome Sequence of Alternaria alternata Isolated from Onion Leaves in South Africa. *Genome Announcements, 4(5).*

Bonants, P. et al., 2010. QBOL: a new EU project focusing on DNA barcoding of Quarantine organisms. EPPO Bulletin, 40(1), pp.30–33.

Capella-Gutiérrez, S., Silla-Martínez, J.M. & Gabaldón, T., 2009. trimAl: a tool for automated alignment trimming in large-scale phylogenetic analyses. Bioinformatics, 25(15), pp.1972–1973.

Cingolani, P. et al., 2012. A program for annotating and predicting the effects of single nucleotide polymorphisms, SnpEff: SNPs in the genome of Drosophila melanogaster strain w1118; iso-2; iso-3. Fly, 6(2), pp.80–92.

Danecek, P. et al., 2011. The variant call format and VCFtools. Bioinformatics, 27(15), pp.2156–2158.

Dang, H.X. et al., 2015. The Alternaria genomes database: a comprehensive resource for a

fungal genus comprised of saprophytes, plant pathogens, and allergenic species. BMC Genomics, 16, p.239.

Dobin, A. et al., 2013. STAR: ultrafast universal RNA-seq aligner. Bioinformatics, 29(1), pp.15–21.

van der Does, H.C. et al., 2016. Transcription factors encoded on core and accessory chromosomes of Fusarium oxysporum induce expression of effector Genes. PLoS Genetics, 12(11), p.e1006401.

Faino, L. et al., 2016. Transposons passively and actively contribute to evolution of the two-speed genome of a fungal pathogen. Genome Research, 26(8), pp.1091–1100.

Gijzen, M., 2009. Runaway repeats force expansion of the Phytophthora infestans genome. Genome Biology, 10(10), p.241.

Glass, N.L. & Kaneko, I., 2003. Fatal attraction: nonself recognition and heterokaryon incompatibility in filamentous fungi. Eukaryotic Cell, 2(1), pp.1–8.

Gurevich, A. et al., 2013. QUAST: quality assessment tool for genome assemblies. Bioinformatics, 29(8), pp.1072–1075.

Harimoto, Y. et al., 2007. Expression profiles of genes encoded by the supernumerary chromosome controlling AM-toxin biosynthesis and pathogenicity in the apple pathotype of Alternaria alternata. Molecular Plant-Microbe Interactions, 20(12), pp.1463–1476.

Harimoto, Y. et al., 2008. Multiple copies of AMT2 are prerequisite for the apple pathotype of Alternaria alternata to produce enough AM-toxin for expressing pathogenicity. Journal of General Plant Pathology, 74(3), pp.222–229.

Hatta, R. et al., 2002. A conditionally dispensable chromosome controls host-specific pathogenicity in the fungal plant pathogen Alternaria alternata. Genetics, 161(1), pp.59–70.

Hoff, K.J. et al., 2016. BRAKER1: Unsupervised RNA-Seq-Based Genome Annotation with GeneMark-ET and AUGUSTUS. Bioinformatics, 32(5), pp.767–769.

Hou, Y. et al., 2016. Comparative genomics of pathogens causing brown spot disease of tobacco: Alternaria longipes and Alternaria alternata. *PLoS One , 11(5), p.e0155258.*

Hu, J. et al., 2012. Genomic characterization of the conditionally dispensable chromosome in Alternaria arborescens provides evidence for horizontal gene transfer. BMC Genomics, 13, p.171.

Huang, L. et al., 2018. dbCAN-seq: a database of carbohydrate-active enzyme (CAZyme) sequence and annotation. Nucleic Acids Research, 46(D1), pp.D516–D521.

Johnson, L.J. et al., 2001. Spontaneous loss of a conditionally dispensable chromosome from the Alternaria alternata apple pathotype leads to loss of toxin production and pathogenicity. Current Genetics, 40(1), pp.65–72.

Johnson, R.D. et al., 2000. Cloning and characterization of a cyclic peptide synthetase gene from Alternaria alternata apple pathotype whose product is involved in AM-toxin synthesis and pathogenicity. Molecular Plant-Microbe Interactions, 13(7), pp.742–753.

Jones, P. et al., 2014. InterProScan 5: genome-scale protein function classification. Bioinformatics, 30(9), pp.1236–1240.

Käll, L., Krogh, A. & Sonnhammer, E.L.L., 2004. A combined transmembrane topology and signal peptide prediction method. Journal of Molecular Biology, 338(5), pp.1027–1036.

Katoh, K. & Standley, D.M., 2013. MAFFT multiple sequence alignment software version 7: improvements in performance and usability. Molecular Biology and Evolution, 30(4), pp.772–780.

Kodama, M. et al., 1998. Host-specific toxin deficient mutants of the tomato pathotype of Alternaria alternata obtained by restriction enzyme-mediated integration. In K. Kohmoto & O. C. Yoder, eds. Molecular Genetics of Host-Specific Toxins in Plant Disease. Developments in plant pathology. Dordrecht: Springer Netherlands, pp. 35–42.

Kohmoto, K. et al., 1976. Multiple host-specific toxins of Alternaria mali and their effect on the permeability of host cells. Physiological Plant Pathology, 8(2), pp.141–153.

Kombrink, A. & Thomma, B.P.H.J., 2013. LysM effectors: secreted proteins supporting fungal life. PLoS Pathogens, 9(12), p.e1003769.

Koren, S. et al., 2017. Canu: scalable and accurate long-read assembly via adaptive k-mer weighting and repeat separation. Genome Research, 27(5), pp.722–736.

Krogh, A. et al., 2001. Predicting transmembrane protein topology with a hidden Markov model: application to complete genomes. Journal of Molecular Biology, 305(3), pp.567–580.

Langmead, B. & Salzberg, S.L., 2012. Fast gapped-read alignment with Bowtie 2. Nature Methods, 9(4), pp.357–359.

Lawrence, D.P. et al., 2013. The sections of Alternaria: formalizing species-group concepts. Mycologia, 105(3), pp.530–546.

Li, H. et al., 2009. The Sequence Alignment/Map format and SAMtools. Bioinformatics, 25(16), pp.2078–2079.

Li, L., Stoeckert, C.J. & Roos, D.S., 2003. OrthoMCL: identification of ortholog groups for eukaryotic genomes. Genome Research, 13(9), pp.2178–2189.

Liu, K., Linder, C.R. & Warnow, T., 2011. RAxML and FastTree: comparing two methods for large-scale maximum likelihood phylogeny estimation. *PLoS One, 6(11), p.e27731.*

Loman, N.J., Quick, J. & Simpson, J.T., 2015. A complete bacterial genome assembled de novo using only nanopore sequencing data. Nature Methods, 12(8), pp.733–735.

Masunaka, A. et al., 2005. An Isolate of Alternaria alternata That Is Pathogenic to Both Tangerines and Rough Lemon and Produces Two Host-Selective Toxins, ACT- and ACR-Toxins. Phytopathology, 95(3), pp.241–247.

Masunaka, A. et al., 2000. Distribution and Characterization of AKT Homologs in the Tangerine Pathotype of Alternaria alternata. Phytopathology, 90(7), pp.762–768.

McKenna, A. et al., 2010. The Genome Analysis Toolkit: a MapReduce framework for analyzing next-generation DNA sequencing data. Genome Research, 20(9), pp.1297–1303.

Mistry, J. et al., 2013. Challenges in homology search: HMMER3 and convergent evolution of coiled-coil regions. Nucleic Acids Research, 41(12), p.e121.

Miyamoto, Y. et al., 2010. ACTTS3 encoding a polyketide synthase is essential for the biosynthesis of ACT-toxin and pathogenicity in the tangerine pathotype of Alternaria alternata. Molecular Plant-Microbe Interactions, 23(4), pp.406–414.

Miyamoto, Y. et al., 2009. Function of genes encoding acyl-CoA synthetase and enoyl-CoA hydratase for host-selective act-toxin biosynthesis in the tangerine pathotype of Alternaria alternata. Phytopathology, 99(4), pp.369–377.

Nakashima, T. et al., 1985. Isolation and structures of AK-toxin I and II. Host-specific phytotoxic metabolites produced by Alternaria alternata Japanese pear pathotype. Agricultural and biological chemistry, 49(3), pp.807–815.

Nguyen, H.D.T. et al., 2016. Draft Genome Sequence of Alternaria alternata ATCC 34957. Genome announcements, 4(1).

Nieuwenhuis, B.P.S. & James, T.Y., 2016. The frequency of sex in fungi. Philosophical Transactions of the Royal Society of London. Series B, Biological Sciences, 371(1706).

Pfeifer, B. et al., 2014. PopGenome: an efficient Swiss army knife for population genomic analyses in R. Molecular Biology and Evolution, 31(7), pp.1929–1936.

Quaedvlieg, W. et al., 2012. DNA barcoding of Mycosphaerella species of quarantine importance to Europe. Persoonia, 29, pp.101–115.

Ruan, J., 2016. Ultra-fast de novo assembler using long noisy reads. Available at: https://github.com/ruanjue/smartdenovo [Accessed June 26, 2018].

Schmidt, S.M. et al., 2013. MITEs in the promoters of effector genes allow prediction of novel virulence genes in Fusarium oxysporum. BMC Genomics, 14, p.119.

Shelest, E., 2017. Transcription Factors in Fungi: TFome Dynamics, Three Major Families, and Dual-Specificity TFs. Frontiers in genetics, 8, p.53.

Simão, F.A. et al., 2015. BUSCO: assessing genome assembly and annotation completeness with single-copy orthologs. Bioinformatics, 31(19), pp.3210–3212.

Smith, I.M. et al., 1997. Quarantine pests for Europe-data sheets on quarantine pests for the European Union and for the European and Mediterranean plant protection Organization. 2. Wallingford: CAB International.

Sperschneider, J. et al., 2016. EffectorP: predicting fungal effector proteins from secretomes using machine learning. The New Phytologist, 210(2), pp.743–761.

Stanke, M. & Morgenstern, B., 2005. AUGUSTUS: a web server for gene prediction in eukaryotes that allows user-defined constraints. Nucleic Acids Research, 33(Web Server issue), pp.W465-7.

Stewart, J.E. et al., 2013. Signatures of recombination in clonal lineages of the citrus brown spot pathogen, Alternaria alternata sensu lato. Phytopathology, 103(7), pp.741–749.

Stumpf, M.P.H. & McVean, G.A.T., 2003. Estimating recombination rates from population-

genetic data. Nature Reviews. Genetics, 4(12), pp.959–968.

Tanaka, A. et al., 1999. Insertional mutagenesis and cloning of the genes required for biosynthesis of the host-specific AK-toxin in the Japanese pear pathotype of Alternaria alternata. Molecular Plant-Microbe Interactions, 12(8), pp.691–702.

Tanaka, A. & Tsuge, T., 2000. Structural and functional complexity of the genomic region controlling AK-toxin biosynthesis and pathogenicity in the Japanese pear pathotype of Alternaria alternata. Molecular Plant-Microbe Interactions, 13(9), pp.975–986.

Testa, A.C. et al., 2015. CodingQuarry: highly accurate hidden Markov model gene prediction in fungal genomes using RNA-seq transcripts. BMC Genomics, 16, p.170.

Thomma, B.P.H.J., 2003. Alternaria spp.: from general saprophyte to specific parasite. Molecular Plant Pathology, 4(4), pp.225–236.

Tsuge, T. et al., 2016. Evolution of pathogenicity controlled by small, dispensable chromosomes in Alternaria alternata pathogens. Physiological and Molecular Plant Pathology, 95, pp.27–31.

Tsuge, T. et al., 2013. Host-selective toxins produced by the plant pathogenic fungus Alternaria alternata. FEMS Microbiology Reviews, 37(1), pp.44–66.

Vaser, R. et al., 2017. Fast and accurate de novo genome assembly from long uncorrected reads. Genome Research, 27(5), pp.737–746.

Walker, B.J. et al., 2014. Pilon: an integrated tool for comprehensive microbial variant detection and genome assembly improvement. Plos One, 9(11), p.e112963.

Wang, M. et al., 2016. Genomic and transcriptomic analyses of the tangerine pathotype of Alternaria alternata in response to oxidative stress. Scientific reports, 6, p.32437.

Wolters, P.J. et al., 2018. Gapless Genome Assembly of the Potato and Tomato Early Blight Pathogen Alternaria solani. Molecular Plant-Microbe Interactions, 31(7), pp.692–694.

Woudenberg, J.H.C. et al., 2015. Alternaria section Alternaria: Species, formae speciales or pathotypes? Studies in mycology, 82, pp.1–21.

Yu, G. et al., 2016. ggtree□: an R package for visualization and annotation of phylogenetic trees with their covariates and other associated data. Methods in ecology and evolution / British Ecological Society.

Zhang, C. et al., 2018. ASTRAL-III: polynomial time species tree reconstruction from partially resolved gene trees. BMC Bioinformatics, 19(Suppl 6), p.153.

Zolan, M.E., 1995. Chromosome-length polymorphism in fungi. Microbiological reviews, 59(4), pp.686–698.

Supporting information

Supp. information 1
Identification of single copy Ascomycete genes in reference *Alternaria* spp. genomes

Supp. information 2
Gene IDs, location and functional annotations of genes in expanded orthogroups between *A. tenuissima* and *A. arborescens*.

Supp. information 3
Gene IDs, location and functional annotations of genes located on CDC contigs from apple and Asian pear pathotype isolates.

Supp. information 4
Toxin gene BLAST hits in publicly available *Alternaria* spp. genomes, allowing identification of pathotype isolates.

Supp. information 5
Additional methods

Figure Legends

Figure 1
Genome alignment between the reference *A. solani* genome and long-read assemblies of *A. alternata* apple (A) and Asian pear (B) pathotypes. Links are shown between aligned regions. Locations of telomere repeat sequences are marked within assembled contigs. Contig order in reference to *A. solani* chromosomes is summarized, with those contigs displaying evidence of structural rearrangement marked with an asterisk.

Figure 2
Distinct DDE and gypsy family transposon families between genomes of *A. arborescens* (arb) and *A. tenuissima* (ten) clade isolates. Numbers of identified transposons are also shown for hAT, TY1 copia, mariner, cacta, LINE, MuDR / Mu transposases, helitrons and the Ant1-like mariner elements.

Figure 3
Phylogeny of sequenced and publicly available *Alternaria* spp. genomes. Maximum parsimony consensus phylogeny of 500 conserved single copy loci. Dotted lines show branches with support from < 80% of trees. Mating type idiomorphs MAT1-1-1 and MAT1-2-1 show distribution throughout the phylogeny. Isolates pathotype is labelled following identification of genes involved in synthesis of apple, pear, strawberry, tangerine, rough lemon and tomato toxins.

Figure 4

Presence/absence of toxin and mating type genes for 89 *Alternaria* isolates. Results are plotted onto the 5-gene phylogeny of Armitage (2015). MAT1-1-1 and MAT1-2-1 mating type idiomorphs are designated.

Figure 5

Number of *Alternaria* lesions per apple leaf at 14 dpi for treatments in virulence assays on *cv.* Spartan or *cv.* Bramley's Seedling leaves. Apple pathotype isolates (*FERA 635*, *FERA 743* and *FERA 1166*) cause significant disease symptoms in comparison to control leaves, in contrast to non-pathotype isolates (*FERA 648*, *FERA 1082* and *FERA 1164*). Number of lesions (±SE) are shown with significance at $P < 0.05$, as determined from a GLM at the isolate and pathotype level.

Table 1

Assembly and gene prediction statistics for genomes from three A. alternata species group lineages, including apple and Asian pear pathotype isolates. Number of genes predicted to encode secreted proteins, secreted effectors (EffectorP) and secreted carbohydrate active enzymes (CAZymes) are shown as well as the total number of secondary metabolite clusters in the genome. The percentage of 1315 conserved ascomycete genes that were identified as complete and present in a single copy within assemblies or gene models are shown.

Table 2

Identification of CDC regions in *A. alternata* apple and Asian pear pathotype reference genomes through read alignment from sequenced isolates. Contigs showing reductions in coverage from non-Asian pear or apple pathotype isolates were identified as regions of conditionally dispensable chromosomes (CDCs).

Table 3

Genomic location of homologs to genes from apple, pear, strawberry, tangerine, rough lemon, and tomato toxin gene clusters. Results from reference genome isolates *FERA 1166* and *FERA 650* indicate toxin clusters are present in multiple copies within the genome. This is supported by identification of multiple AMT1 homologs in *FERA 635* and *FERA 743*. Homologs are identified by e-value $< 1x10^{-30}$, > 70% query alignment. Homology between query sequences is shown (homolog groups), as determined from reciprocal BLAST searches between queries.

Table 4

NCBI biosample and genome accession numbers of data generated in this study.

A

A. solani NL03003

Apple pathotype FERA 1166

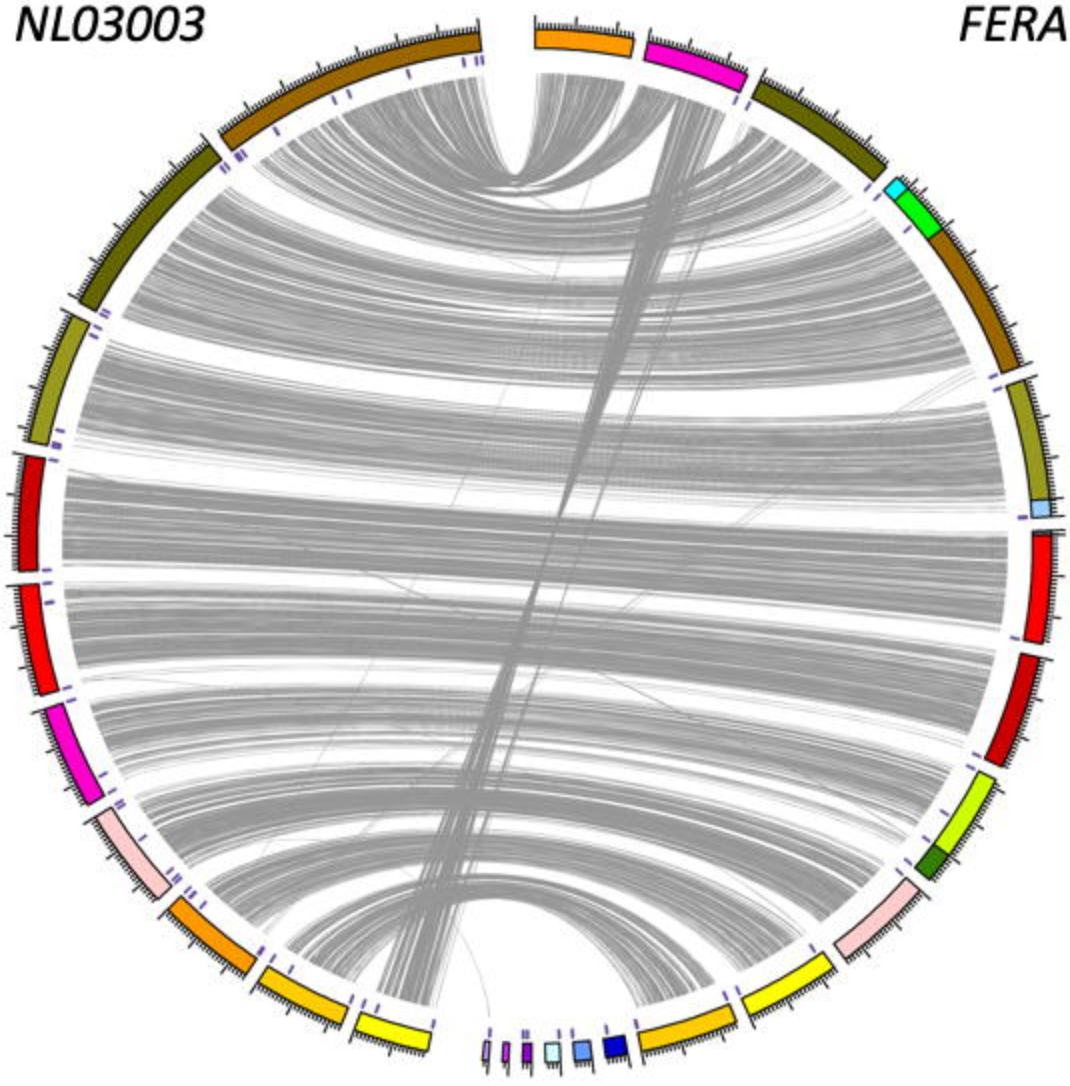

NL03003 chromosome	*FERA 1166* contig
1	8, 6*, 2
2	17, 12, 1
3	3, 16
4	22, 5
5	4
6	11, 13
7	7
8	10
9	9
10	6*
-	14, 15, 18, 19, 20, 21

B

A. solani NL03003

Asian pear pathotype FERA 650

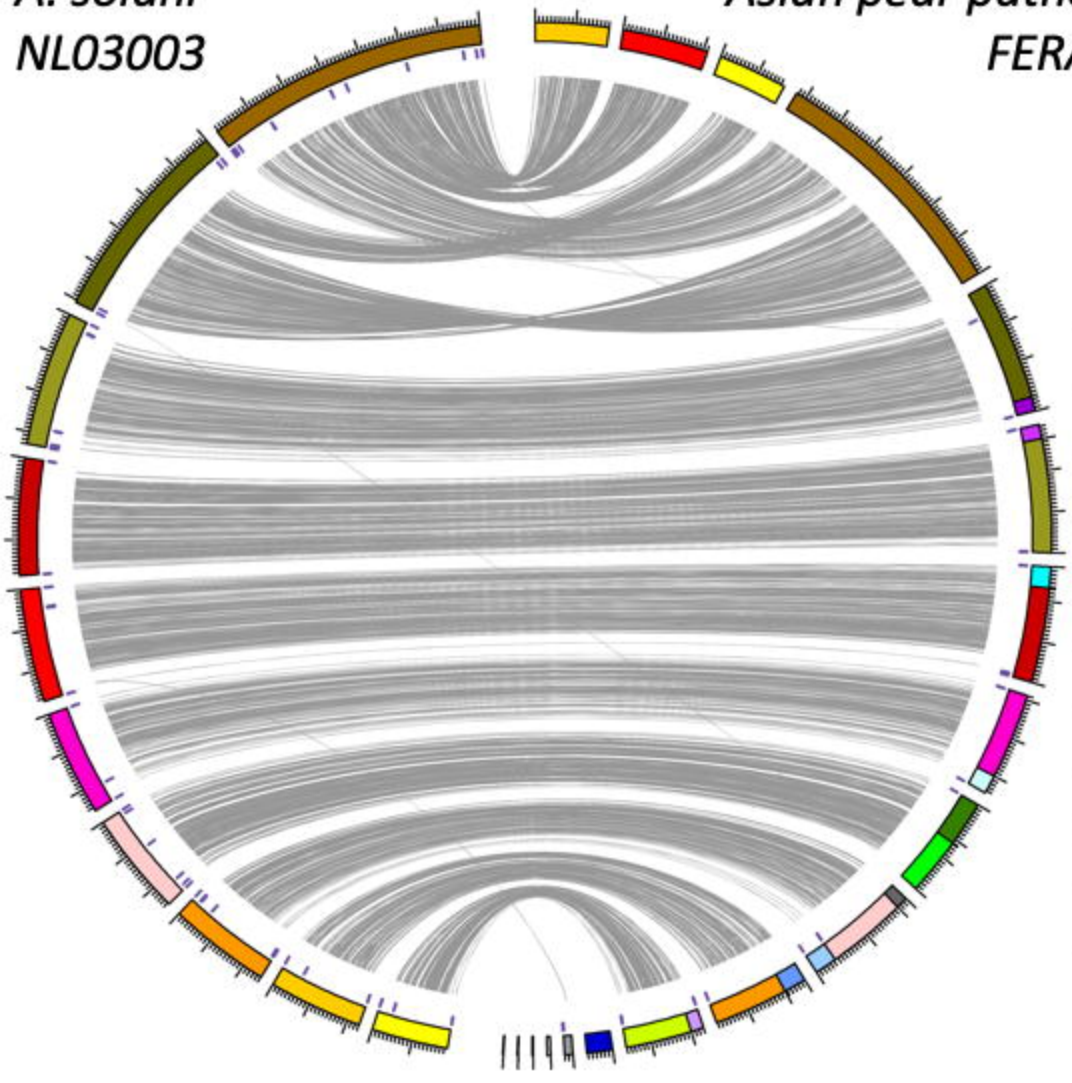

NL03003 chromosome	*FERA 650* contig
1	9, 5, 1*
2	10, 1*
3	2, 19
4	20, 3
5	17, 4
6	6, 18
7	13, 12
8	22, 7, 16
9	15, 8
10	21, 11
-	14, 23, 24, 25, 26, 27

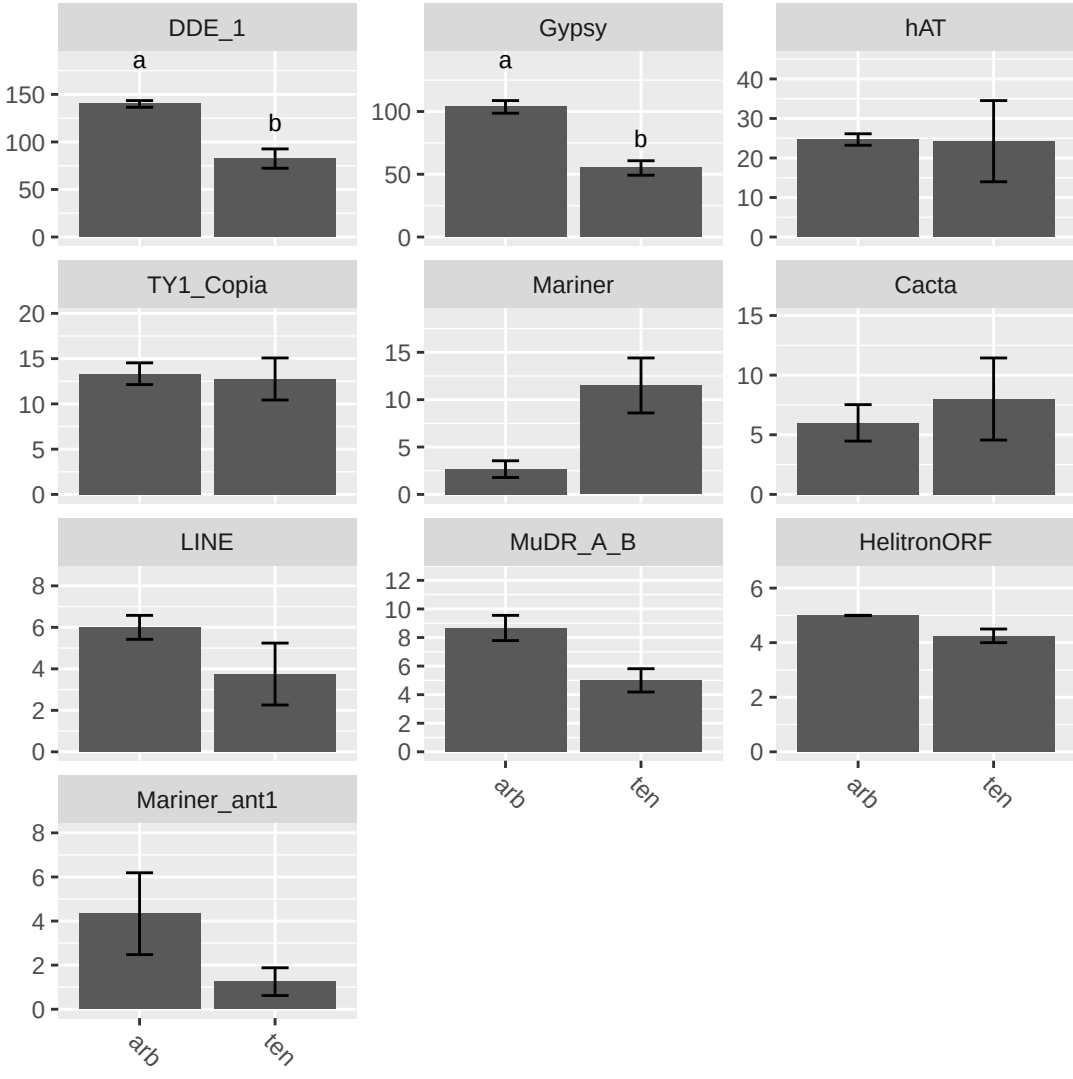
DDE_1
a
b
150
100
50
0
Gypsy
a
b
100
50
0
hAT
40
30
20
10
0
TY1_Copia
20
15
10
5
0
Mariner
15
10
5
0
Cacta
15
10
5
0
LINE
8
6
4
2
0
MuDR_A_B
12
10
8
6
4
2
0
arb
ten
HelitronORF
6
4
2
0
arb
ten
Mariner_ant1
8
6
4
2
0
arb
ten

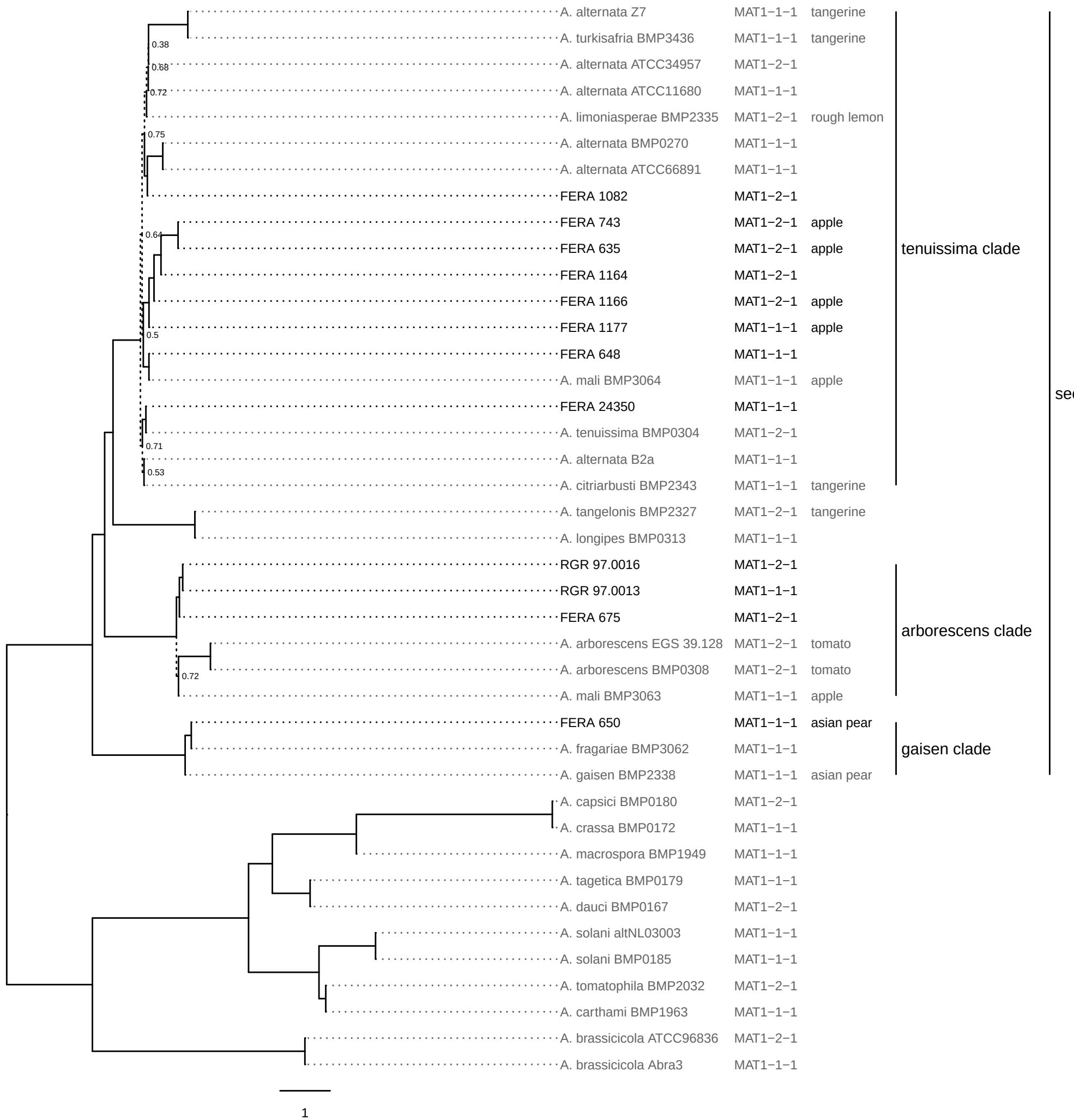
A. alternata Z7 MAT1−1−1 tangerine
A. turkisafria BMP3436 MAT1−1−1 tangerine
A. alternata ATCC34957 MAT1−2−1
A. alternata ATCC11680 MAT1−1−1
A. limoniasperae BMP2335 MAT1−2−1 rough lemon
A. alternata BMP0270 MAT1−1−1
A. alternata ATCC66891 MAT1−1−1
FERA 1082 MAT1−2−1
FERA 743 MAT1−2−1 apple
FERA 635 MAT1−2−1 apple
FERA 1164 MAT1−2−1
FERA 1166 MAT1−2−1 apple
FERA 1177 MAT1−1−1 apple
FERA 648 MAT1−1−1
A. mali BMP3064 MAT1−1−1 apple
FERA 24350 MAT1−1−1
A. tenuissima BMP0304 MAT1−2−1
A. alternata B2a MAT1−1−1
A. citriarbusti BMP2343 MAT1−1−1 tangerine
A. tangelonis BMP2327 MAT1−2−1 tangerine
A. longipes BMP0313 MAT1−1−1
RGR 97.0016 MAT1−2−1
RGR 97.0013 MAT1−1−1
FERA 675 MAT1−2−1
A. arborescens EGS 39.128 MAT1−2−1 tomato
A. arborescens BMP0308 MAT1−2−1 tomato
A. mali BMP3063 MAT1−1−1 apple
FERA 650 MAT1−1−1 asian pear
A. fragariae BMP3062 MAT1−1−1
A. gaisen BMP2338 MAT1−1−1 asian pear
A. capsici BMP0180 MAT1−2−1
A. crassa BMP0172 MAT1−1−1
A. macrospora BMP1949 MAT1−1−1
A. tagetica BMP0179 MAT1−1−1
A. dauci BMP0167 MAT1−2−1
A. solani altNL03003 MAT1−1−1
A. solani BMP0185 MAT1−1−1
A. tomatophila BMP2032 MAT1−2−1
A. carthami BMP1963 MAT1−1−1
A. brassicicola ATCC96836 MAT1−2−1
A. brassicicola Abra3 MAT1−1−1
0.38
0.68
0.72
0.75
0.64
0.5
0.71
0.53
0.72
tenuissima clade
arborescens clade
gaisen clade
sect. Alternaria
1

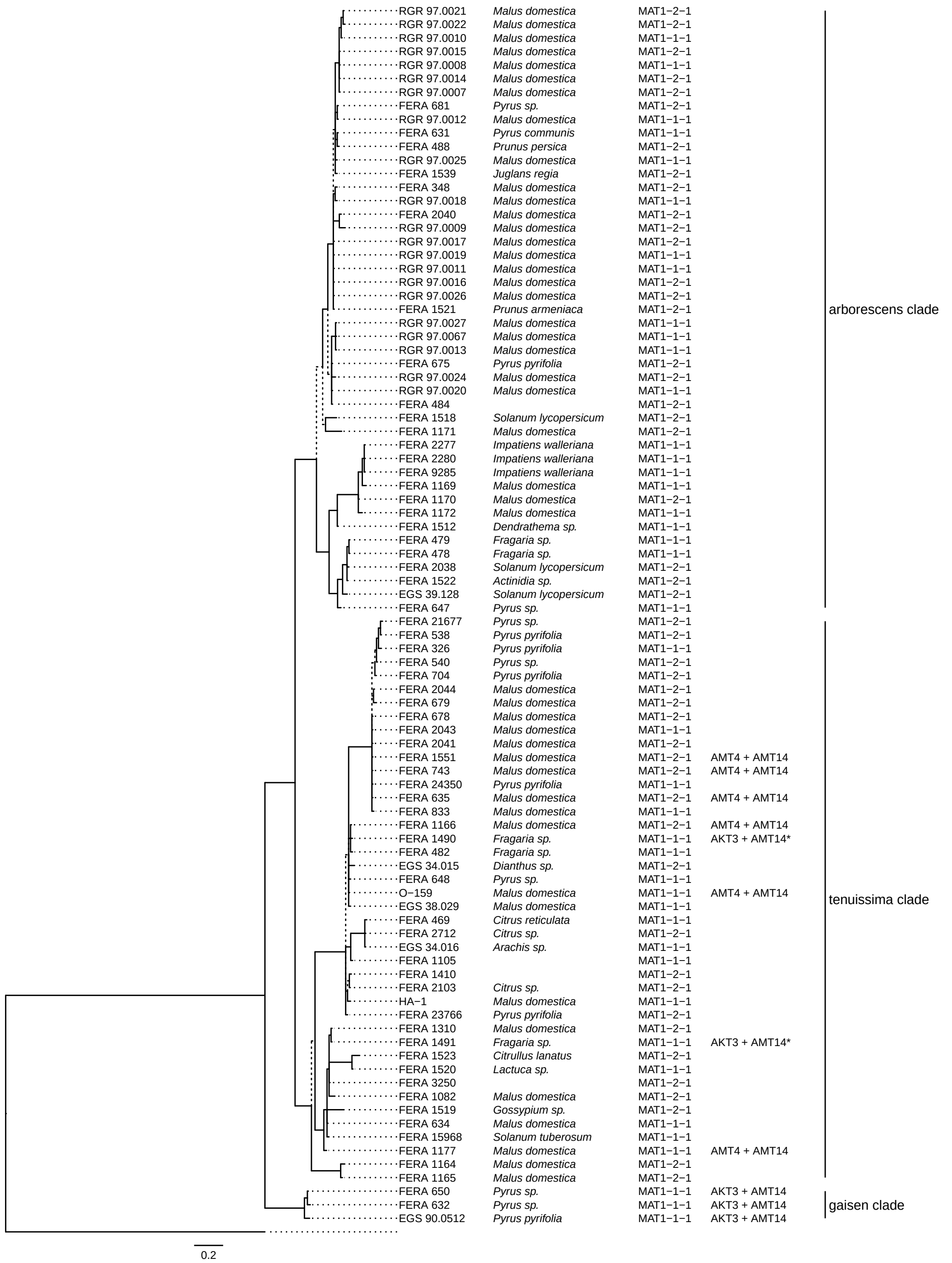
RGR 97.0021 Malus domestica MAT1−2−1
RGR 97.0022 Malus domestica MAT1−2−1
RGR 97.0010 Malus domestica MAT1−1−1
RGR 97.0015 Malus domestica MAT1−2−1
RGR 97.0008 Malus domestica MAT1−1−1
RGR 97.0014 Malus domestica MAT1−2−1
RGR 97.0007 Malus domestica MAT1−2−1
FERA 681 Pyrus sp. MAT1−2−1
RGR 97.0012 Malus domestica MAT1−1−1
FERA 631 Pyrus communis MAT1−1−1
FERA 488 Prunus persica MAT1−2−1
RGR 97.0025 Malus domestica MAT1−1−1
FERA 1539 Juglans regia MAT1−2−1
FERA 348 Malus domestica MAT1−2−1
RGR 97.0018 Malus domestica MAT1−1−1
FERA 2040 Malus domestica MAT1−2−1
RGR 97.0009 Malus domestica MAT1−2−1
RGR 97.0017 Malus domestica MAT1−2−1
RGR 97.0019 Malus domestica MAT1−1−1
RGR 97.0011 Malus domestica MAT1−1−1
RGR 97.0016 Malus domestica MAT1−2−1
RGR 97.0026 Malus domestica MAT1−2−1
FERA 1521 Prunus armeniaca MAT1−2−1
RGR 97.0027 Malus domestica MAT1−1−1
RGR 97.0067 Malus domestica MAT1−1−1
RGR 97.0013 Malus domestica MAT1−1−1
FERA 675 Pyrus pyrifolia MAT1−2−1
RGR 97.0024 Malus domestica MAT1−2−1
RGR 97.0020 Malus domestica MAT1−1−1
FERA 484 MAT1−2−1
FERA 1518 Solanum lycopersicum MAT1−2−1
FERA 1171 Malus domestica MAT1−2−1
FERA 2277 Impatiens walleriana MAT1−1−1
FERA 2280 Impatiens walleriana MAT1−1−1
FERA 9285 Impatiens walleriana MAT1−1−1
FERA 1169 Malus domestica MAT1−1−1
FERA 1170 Malus domestica MAT1−2−1
FERA 1172 Malus domestica MAT1−1−1
FERA 1512 Dendrathema sp. MAT1−1−1
FERA 479 Fragaria sp. MAT1−1−1
FERA 478 Fragaria sp. MAT1−1−1
FERA 2038 Solanum lycopersicum MAT1−2−1
FERA 1522 Actinidia sp. MAT1−2−1
EGS 39.128 Solanum lycopersicum MAT1−2−1
FERA 647 Pyrus sp. MAT1−1−1
FERA 21677 Pyrus sp. MAT1−2−1
FERA 538 Pyrus pyrifolia MAT1−2−1
FERA 326 Pyrus pyrifolia MAT1−1−1
FERA 540 Pyrus sp. MAT1−2−1
FERA 704 Pyrus pyrifolia MAT1−2−1
FERA 2044 Malus domestica MAT1−2−1
FERA 679 Malus domestica MAT1−2−1
FERA 678 Malus domestica MAT1−2−1
FERA 2043 Malus domestica MAT1−1−1
FERA 2041 Malus domestica MAT1−2−1
FERA 1551 Malus domestica MAT1−2−1 AMT4 + AMT14
FERA 743 Malus domestica MAT1−2−1 AMT4 + AMT14
FERA 24350 Pyrus pyrifolia MAT1−1−1
FERA 635 Malus domestica MAT1−2−1 AMT4 + AMT14
FERA 833 Malus domestica MAT1−1−1
FERA 1166 Malus domestica MAT1−2−1 AMT4 + AMT14
FERA 1490 Fragaria sp. MAT1−1−1 AKT3 + AMT14*
FERA 482 Fragaria sp. MAT1−1−1
EGS 34.015 Dianthus sp. MAT1−2−1
FERA 648 Pyrus sp. MAT1−1−1
O−159 Malus domestica MAT1−1−1 AMT4 + AMT14
EGS 38.029 Malus domestica MAT1−1−1
FERA 469 Citrus reticulata MAT1−1−1
FERA 2712 Citrus sp. MAT1−2−1
EGS 34.016 Arachis sp. MAT1−1−1
FERA 1105 MAT1−1−1
FERA 1410 MAT1−2−1
FERA 2103 Citrus sp. MAT1−2−1
HA−1 Malus domestica MAT1−1−1
FERA 23766 Pyrus pyrifolia MAT1−2−1
FERA 1310 Malus domestica MAT1−2−1
FERA 1491 Fragaria sp. MAT1−1−1 AKT3 + AMT14*
FERA 1523 Citrullus lanatus MAT1−2−1
FERA 1520 Lactuca sp. MAT1−1−1
FERA 3250 MAT1−2−1
FERA 1082 Malus domestica MAT1−2−1
FERA 1519 Gossypium sp. MAT1−2−1
FERA 634 Malus domestica MAT1−1−1
FERA 15968 Solanum tuberosum MAT1−1−1
FERA 1177 Malus domestica MAT1−1−1 AMT4 + AMT14
FERA 1164 Malus domestica MAT1−2−1
FERA 1165 Malus domestica MAT1−2−1
FERA 650 Pyrus sp. MAT1−1−1 AKT3 + AMT14
FERA 632 Pyrus sp. MAT1−1−1 AKT3 + AMT14
EGS 90.0512 Pyrus pyrifolia MAT1−1−1 AKT3 + AMT14
arborescens clade
tenuissima clade
gaisen clade
0.2

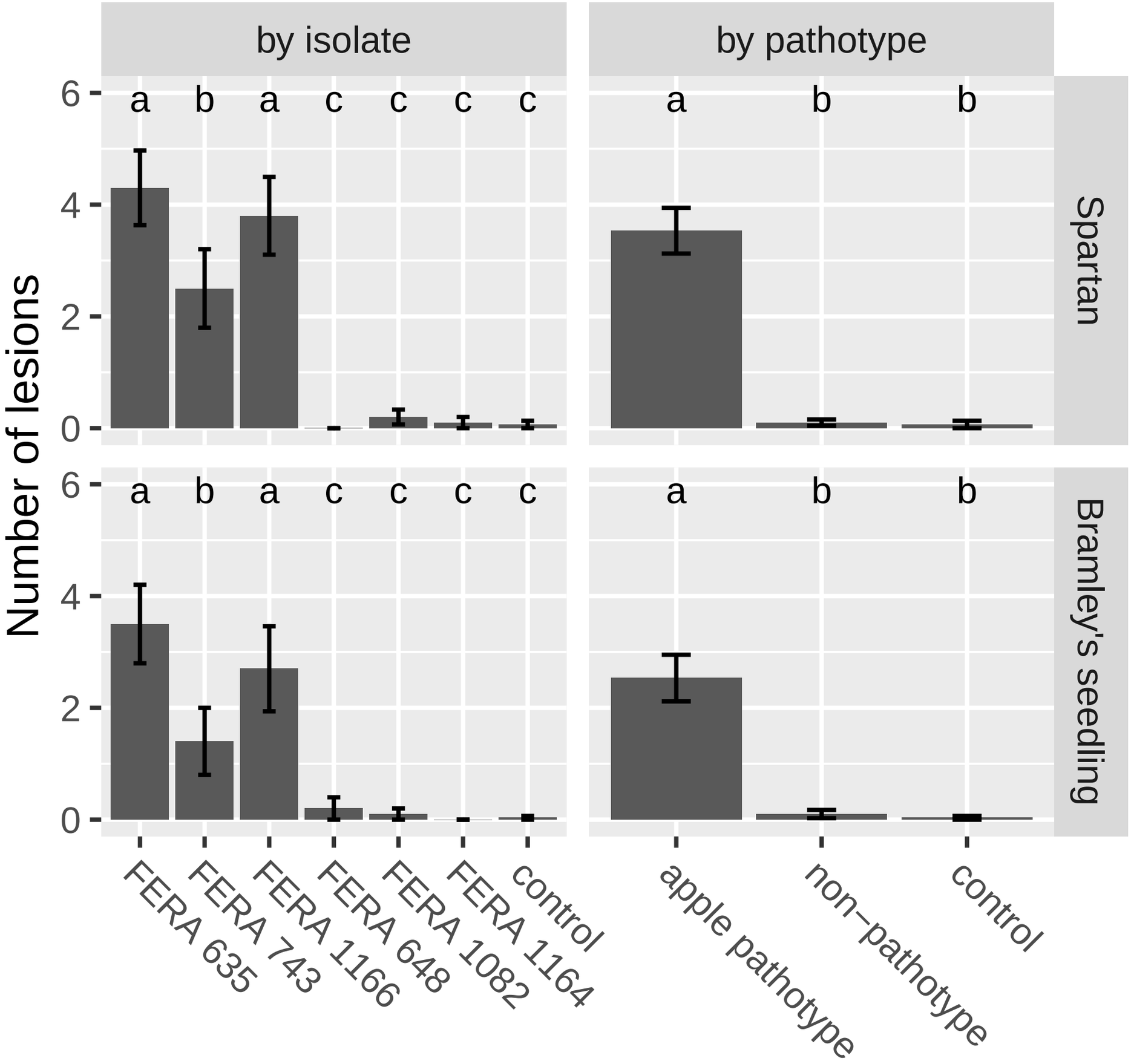
by isolate
by pathotype
Spartan
Bramley's seedling
Number of lesions
0
2
4
6
a b a c c c c
a b b
FERA 635
FERA 743
FERA 1166
FERA 648
FERA 1082
FERA 1164
control
apple pathotype
non−pathotype
control

Organism	*A. gaisen*	*A. tenuissima*								*A. arborescens*		
Pathotype	pear	apple				non-pathotype				non-pathotype		
Isolate	FERA 650	FERA 1166	FERA 635	FERA 743	FERA 1177	FERA 648	FERA 1082	FERA 1164	FERA 24350	FERA 675	RGR 97.0013	RGR 97.0016
Assembly size (Mb)	34.3	35.7	36.1	35.9	35.6	33.5	33.9	34.7	33.0	33.9	33.8	33.8
Contigs	27	22	912	788	735	124	345	250	167	325	287	339
Largest contig (Mb)	6.26	3.90	1.43	3.88	4.61	3.50	1.72	2.04	1.90	2.09	1.61	1.06
N50 (Kb)	2,110	1,584	319	622	537	1,341	547	709	608	862	685	528
Repeatmasked (Kb)	749	1,268	953	869	865	658	628	983	466	853	955	784
Repeatmasked (%)	2.18	3.55	2.64	2.42	2.43	1.96	1.85	2.83	1.41	2.51	2.83	2.32
Conserved Ascomycete genes in genome (%)	98.7	99.0	98.8	98.9	98.8	99.0	98.6	98.8	99.0	98.6	98.6	98.7
Total genes	13169	13576	13733	13707	13580	12757	13028	13114	12806	12896	12766	12820
Total proteins	13220	13633	13812	13776	13647	12798	13091	13169	12856	12936	12813	12863
Conserved Ascomycete genes in gene models (%)	98.7	99.0	98.1	98.2	97.7	98.3	98.2	98.5	98.4	97.7	98.1	98.1
Secreted proteins	1208	1251	1261	1247	1270	1228	1246	1235	1225	1199	1189	1185
Secreted EffectorP proteins	246	248	264	263	268	233	252	252	241	236	229	229
Secreted CAZYme proteins	383	389	397	390	397	392	401	385	391	375	372	382
Secondary metabolite clusters	30	34	36	36	30	28	30	29	26	28	28	30

Reference Genome	Reference contig	Length (bp)	*A. gaisen* pear	*A. tenuissima*								*A. arborescens*		
				apple				-				-		
			FERA 650	FERA 1166	FERA 635	FERA 743	FERA 1177	FERA 648	FERA 1082	FERA 1164	FERA 24350	FERA 675	RGR 97.0013	RGR 97.0016
FERA 1166	1	3902980	32	49	26	40	60	34	21	28	36	53	35	26
	2	3781932	31	49	26	40	58	33	20	29	35	51	34	26
	3	3000390	33	50	26	40	59	34	21	28	36	53	35	26
	4	2851745	32	49	27	41	59	34	21	28	36	53	36	27
	5	2693844	33	49	27	40	60	34	21	29	36	53	36	27
	6	2583941	33	50	27	40	60	34	21	29	36	53	36	27
	7	2502671	33	49	26	40	59	34	21	28	36	52	35	26
	8	2455819	32	49	27	40	60	33	21	29	35	52	35	26
	9	2451092	32	49	26	40	59	33	20	28	35	52	35	26
	10	2402550	31	49	26	40	58	32	21	28	35	51	34	25
	11	2194253	32	49	26	40	59	34	21	28	35	52	35	26
	12	1303685	33	49	27	40	59	34	21	28	36	53	36	27
	13	767820	23	48	24	36	47	25	17	25	29	44	26	20
	14 (CDC)	549494	0	81	29	79	115	0	23	33	0	0	0	0
	15 (CDC)	435297	62	90	51	79	407	0	0	0	0	0	0	0
	16	433285	23	48	26	40	53	26	18	28	33	51	27	20
	17	391795	26	48	20	33	56	30	19	27	29	51	30	23
	18 (CDC)	368761	0	49	22	40	32	0	0	0	0	0	0	0
	19 (CDC)	225742	0	48	22	61	72	0	18	31	0	0	0	0
	20 (CDC)	154051	0	69	20	45	214	0	0	0	0	0	0	0
	21 (CDC)	143777	0	49	20	36	219	0	0	0	0	0	0	0
	22	109256	25	50	20	30	50	26	14	22	30	35	27	22
FERA 650	1	6257968	35	43	25	38	58	33	20	28	35	50	34	26
	2	2925786	35	45	25	39	58	34	20	28	35	51	35	26

3	2776589	35	44	26	39	58	34	20	28	35	51	35	26
4	2321443	35	45	26	39	58	34	20	28	35	51	35	27
5	2116911	35	46	26	40	59	35	21	29	36	52	36	27
6	2110033	35	44	25	39	58	33	20	28	35	51	35	26
7	1975041	35	42	25	38	56	33	19	27	34	50	34	26
8	1822907	35	43	25	39	58	33	20	28	35	51	35	26
9	1811374	34	42	25	38	57	32	19	27	34	49	34	25
10	1696734	34	42	25	38	56	32	19	27	34	50	34	26
11	1617057	35	43	25	38	57	33	19	27	34	50	34	26
12	1416541	35	47	26	40	60	35	21	29	36	53	36	27
13	1110254	35	39	24	36	55	31	19	26	33	48	32	24
14 (CDC)	629968	68	49	21	41	202	0	0	0	0	0	0	0
15	554254	34	40	24	37	56	32	19	27	33	48	33	25
16 (CDC)	547262	34	8	13	18	22	8	5	14	11	20	8	6
17	522351	35	37	23	35	55	31	18	26	33	47	33	24
18	463030	34	30	22	33	49	25	17	24	29	44	28	21
19	353531	34	30	21	34	49	26	16	23	30	43	28	21
20	350965	34	20	18	27	45	22	15	19	26	40	20	18
21	313768	35	24	19	29	46	25	15	22	27	38	28	19
22	288922	33	35	23	35	51	28	21	24	31	44	30	22
23 (CDC)	206183	34	1	3	5	43	0	0	10	1	0	0	0
24 (CDC)	89891	70	0	0	0	0	0	0	0	0	0	0	0
25	25201	16	0	0	0	0	0	0	0	0	0	0	0
26	23394	5	0	0	0	0	0	0	0	0	0	0	0
27	19592	17	0	0	0	0	0	0	0	0	0	0	0

Pathotype	Gene	NCBI Accession	Group	*A. tenuissima* apple				*A. gaisen* pear
				FERA 635	FERA 743	FERA 1166	FERA 1177	FERA 650
Apple	AMT1	AB525198		201,224	146,160	20, 21	81	
	AMT2	AB525198	a	224	160	20, 21	81	
	AMT3	AB525198		224	160	21	81	
	AMT4	AB525198		178	140	20, 21	81	
	AMT5	AB525198		178	140	20, 21	81	
	AMT6	AB525198		178	140	20, 21	81	
	AMT7	AB525198		178	140	20, 21	81	
	AMT8	AB525198		178	140	20, 21	81	
	AMT9	AB525198		178	140	20, 21	81	
	AMT10	AB525198		178	143	20	81	
	AMT11	AB525198		*199**	*144**	*21**	*81**	
	AMT12	AB525198		199	144	20	129	
	AMT13	AB525198		200	129	20	128	
	AMT14	AB525198		200	129	20	128	14
	AMT15	AB525198				*18***		14*
	AMT16	AB525198		200, 12	129, 13	20, 7	128, 21	12
	AMTR1	AB525198		230	143	20	81	14
Pear	AKT1	AB015351	b					14, 24
	AKT2	AB015352	c					14
	AKT3	AB035492	d					14, 24
	AKTR	AB035491	e					14, 24
Strawberry	AFT1-1	AB070711	b					14, 24
	AFT3-1	AB070713	d					14, 24
	AFT3-2	AB179766	d					14, 24
	AFT9-1	AB179766						14, 24
	AFT10-1	AB179766						14, 24
	AFT11-1	AB179766						14, 24
	AFT12-1	AB179766						24
	AFTS1	AB119280	a	224	160	20, 21	81	
	AFTR-1	AB070712	e					14, 24
	AFTR-2	AB179766	e					14, 24
Tangerine	ACTT1	AB034586	b					14, 24
	ACTT2	AB432914	c					14
	ACTT3	AB176941	d					14, 24
	ACTTR	AB176941	e					14, 24
	ACTT5	AB444613						24
	ACTT6	AB444614						14
Rough Lemon	ACRTS1	AB688098						
	ACRTS2	AB725683						

Tomato	ALT1	AB465676	

Isolate	BioSample	Accession
FERA 675	SAMN06205217	PDUP00000000
RGR 97.0013	SAMN06205218	PDWY00000000
RGR 97.0016	SAMN06205219	PEJP00000000
FERA 650	SAMN06205220	PDWZ00000000
FERA 1082	SAMN06205221	PDXA00000000
FERA 1164	SAMN06205222	PDXB00000000
FERA 1166	SAMN06205223	PDXC00000000
FERA 1177	SAMN06205224	PDXD00000000
FERA 24350	SAMN06205225	PDXE00000000
FERA 635	SAMN06205226	PDXF00000000
FERA 648	SAMN06205227	PDXG00000000
FERA 743	SAMN06205228	PDXH00000000